Towards resource-efficient washing within the continuous vacuum screw filter

Marc Peter Meier, Daniela Anna Rysch, Kerstin Wohlgemuth

Separation and Purification Technology 407 (2026) 139106

Contents lists available at ScienceDirect

Separation and Purification Technology

journal homepage: www.elsevier.com/locate/seppur

Towards resource-efficient washing within the continuous vacuum screw filter

Marc Peter Meier [a,b], Daniela Anna Rysch [a], Kerstin Wohlgemuth [a,b,*]

[a] Laboratory of Plant and Process Design, Department of Biochemical and Chemical Engineering, TU Dortmund University, D-44227 Dortmund, Germany
[b] Institute for Pharmaceutics and Biopharmaceutics, Department of Mathematics and Natural Sciences, Heinrich Heine University Düsseldorf, D-40225 Düsseldorf, Germany

ARTICLE INFO

Keywords:
Continuous manufacturing
Small-scale production
Continuous particle isolation
Continuous vacuum screw filter
Washing efficiency
Wash curve

ABSTRACT

Continuous manufacturing offers substantial potential for process intensification in pharmaceutical production, including improved product quality, reduced waste, and enhanced flexibility. While continuous crystallization technologies are well established, continuous particle isolation remains a bottleneck for realizing end-to-end continuous crystal process chains. To address this gap, the modular continuous vacuum screw filter was developed integrating continuous filtration, washing, and drying.

In this study, the two-stage washing process within this apparatus was systematically optimized for particles in the size range of 355–560 µm with the objective of minimizing washing liquid consumption while fulfilling the requirements for continuous particle isolation, including high purification performance to residual impurity loading of less than 5 ppm, residual moisture below 1%, and maintenance of the particle size distribution. Based on wash curve analysis, various washing liquid dosing units were evaluated with respect to washing efficiency. The results demonstrate that capillary-based dosing units provide significantly higher washing efficiency than nozzle-based dosing units due to gentler application of the washing liquid to the filter cake surface. Using a capillary with circular outlet, the washing liquid consumption in each washing step was reduced by 80%, corresponding to a wash ratio of 4, while achieving the product quality specifications.

Overall, optimization of the two-stage washing process enabled a substantial reduction in washing liquid consumption, improved product quality in terms of product purity and residual moisture, as well as elimination

Abbreviations: API, Active pharmaceutical ingredient; BB, Brilliant blue; CC, Capillary with circular outlet geometry; CH, Chromotrope; CM, Continuous manufacturing; CO, Capillary with oval outlet geometry; CPC, Crystal process chain; CQA, Critical quality attribute; CVSF, Continuous Vacuum Screw Filter; F, Filtration; FW, Filtration and single-stage washing; FWW, Filtration and two-stage washing; HC 0.54, Hollow cone nozzle 0.54; HC 0.85, Hollow cone nozzle 0.85; PSD, Particle size distribution; PTFE, Polytetrafluoroethylene; α, Filling degree / %; Ag_3, Volume-based agglomeration degree / %; $Ag_{3,in}$, Volume-based agglomeration degree of particles entering the CVSF / %; $Ag_{3,out}$, Volume-based agglomeration degree of particles leaving the CVSF / %; c^*_{Ala}, Saturation concentration of L-alanine / g g^{-1}; Δp, Pressure drop / mbar; ΔT, Temperature increase preheater / K; $d_{50,3,in}$, Volume-based median particle diameter of particles entering the CVSF / µm; $d_{50,3,out}$, Volume-based median particle diameter of particles leaving the CVSF / µm; $d_{90-10,3,in}$, Volume-based particle size distribution width of particles entering the CVSF / µm; $d_{90-10,3,out}$, Volume-based particle size distribution width of particles leaving the CVSF / µm; d_i, Inner shaft diameter / mm; $d_{i,module}$, Inner module diameter / mm; d_o, Outer screw diameter / mm; d_{out}, Outlet diameter dosing unit / mm; d_p, Equivalent particle diameter / µm; ε, Porosity of filter cake / %; f_{VP}, Vacuum pump frequency / Hz; L_{screw}, Screw length / mm; $m_{BB,i}$, Mass of brilliant blue after process step I / mg; m_{liquid}, Mass of liquid / g; m_{solid}, Mass of solid / g; $m_{solid,Ala,i}$, Mass of solid L-alanine after process step I / g; n_{screw}, Rotational screw speed / rpm; N_{flight}, Number of flights / -; P, Pitch distance / mm; PSD_{in}, Particle size distribution of particles entering the CVSF; PSD_{out}, Particle size distribution of particles leaving the CVSF; ϕ_{RM}, Residual moisture of particles/ %; Q_3, Volume-based cumulative distribution function / -; Q_{pore}, Volume flow rate of pores / mL min^{-1}; Q_{susp}, Volume flow rate of suspension / mL min^{-1}; Q_{WL}, Volume flow rate of washing liquid / mL min^{-1}; $Q_{WL,1}$, Volume flow rate of washing liquid in the first washing step / mL min^{-1}; $Q_{WL,2}$, Volume flow rate of washing liquid in the second washing step / mL min^{-1}; θ, Spray angle / °; ϑ, Temperature / °C; ρ_{solid}, Density of solid / kg m^{-3}; $V_{non-single\ particles}$, Volume of non-single particles / cm^3; V_{pore}, Volume of pores / cm^3; $V_{single\ particles}$, Volume of single particles / cm^3; V_{WL}, Volume of washing liquid / cm^3; $v_{WL,1}$, Washing liquid velocity in the first washing step / m s^{-1}; WR, Wash ratio / -; WR_1, Wash ratio in the first washing step / -; WR_2, Wash ratio in the second washing step / -; WR_{crit}, Critical wash ratio / -; w_{blade}, Blade width / mm; w_{solid}, Solid weight fraction / wt.-%; $X_{BB,0}$, Initial brilliant blue mass loading in suspension / ppm; $X_{BB,i}$, Brilliant blue mass loading after process step i / ppm; $X^*_{BB,i}$, Mass loading ratio regarding brilliant blue after process step i / %; X^*_{crit}, Critical mass loading ratio / %.

* Corresponding author.
E-mail addresses: marc.meier@tu-dortmund.de (M.P. Meier), kerstin.wohlgemuth@hhu.de (K. Wohlgemuth).

https://doi.org/10.1016/j.seppur.2026.139106
Received 22 April 2026; Received in revised form 25 June 2026; Accepted 26 June 2026
Available online 27 June 2026

of an additional drying step, highlighting the ecological and economic potential of the continuous vacuum screw filter for continuous particle isolation.

1. Introduction

Continuous manufacturing (CM) has gained increasing attention in the pharmaceutical industry due to its potential for process intensification, including the elimination of batch-to-batch variability [1,2], enhanced space-time yield [3,4], and improved process safety [4,5]. Moreover, CM enables reductions in plant volume [6] and process footprint [3,4,6], as well as in investment and production costs [3,7–10], and time-to-market [1,2], while consistently ensuring high product quality [3,7–10]. Furthermore, CM is characterized by the ability to adjust production capacity via operating time, resulting in a smaller equipment footprint compared to conventional batch technologies. Consequently, higher production capacities can be achieved by numbering-up rather than scale-up, thereby avoiding typical scale-up challenges. This flexibility enables the use of CM equipment for both research and development and commercial manufacturing [1,10–13] for production scales ranging from 250 to 1000 kg a^{-1}. As a result, there is a growing demand for compact, flexible, and efficient CM equipment for small-scale production [12].

The crystal process chain (CPC) is involved in more than 90% of active pharmaceutical ingredient (API) primary manufacturing processes. The CPC is downstream of the API synthesis and any required purification steps and starts with the crystallization step. More details concerning the CPC and the state of the art of continuous small-scale crystallization as well as particle isolation technologies can be found in our previous publication [14].

We addressed the lack of technology in the field of continuous small-scale particle isolation with the modular continuous vacuum screw filter (CVSF). The CVSF is patented by TU Dortmund University and combines the process steps filtration, washing, and drying in a flexible, modular setup [15]. The modular design allows flexible adaptation of the apparatus or process to varying input conditions such as suspension properties and substance systems [16,17]. The CVSF must fulfill the requirements for continuous particle isolation, including product purity specifications, the production of dry, free-flowing particles, the maintenance of particle properties or the particle size distribution (PSD) throughout the particle isolation process, and traceability of the solid phase within the apparatus. More information on the concept, working principle, and tested operating windows of the CVSF are provided in our previous publications [14,16].

Within a CPC, a two-stage washing process as part of the particle isolation step is essential to ensure that all critical quality attributes (CQAs) of the final solid product are achieved. The first displacement washing step aims to remove residual mother liquor from the pore system of the filter cake following the preceding crystallization and filtration steps, thereby purifying the product particles to the desired purity. Consequently, the selected washing liquid must satisfy several requirements: it must be miscible with the pore liquid, exhibit a high solubility for the impurities, and must not act as a pure antisolvent in order to avoid inducing supersaturation of the remaining mother liquor, which could otherwise alter the PSD. In addition, the washing liquid should not dissolve the product crystals, as this would result in product loss and may promote agglomeration during the washing process. The subsequent second washing step focuses on the removal of residual washing liquid retained within the pore system of the filter cake following the first washing step. Since the mother liquor has already been effectively displaced, a pure antisolvent can be employed in this step. Moreover, volatile antisolvents are preferred, as their efficient evaporation enables a significant reduction in the residual moisture content of the product particles already at the end of the second washing step.

This study aims to systematically optimize the two-stage washing process with respect to washing liquid consumption and washing efficiency. The objective is to reduce washing liquid consumption and waste generation while maintaining or improving product quality. Moreover, optimizing the two-stage washing process seeks to minimize residual moisture to an extent that may eliminate the need for an additional energy-intensive drying step, while ensuring compliance with all CQAs.

In the context of filter cake washing, washing efficiency is evaluated based on wash curves, which relate particle purification to the specific washing liquid consumption. Here, the specific washing liquid consumption is described by the wash ratio *WR* according to Eq. (1).

$$WR = \frac{V_{WL}}{V_{pore}} = \frac{Q_{WL}}{Q_{pore}} \tag{1}$$

In Eq. (1), V_{WL} or Q_{WL} denote the volume (batch) or volume flow rate (continuous) of the applied washing liquid, respectively. And V_{pore} or Q_{pore} describe the pore volume (batch) and the pore volume flow rate (continuous) of the filter cake to be washed.

In the established two-stage washing process, hollow cone nozzles are used as dosing units for the application of the washing liquids in each step at a set washing liquid volume flow rate of 15 mL min^{-1}. This results in a wash ratio of approximately 20 in each washing step, being significantly higher compared to common wash ratios in industrial washing processes of 1.5–4 [18]. However, the wash ratio required for the washing process depends specifically on the purity requirements of the product. Accordingly, optimization of the two-stage washing process within the CVSF offers significant potential for reducing washing liquid consumption and, consequently, lowering both operational costs and the ecological footprint.

Hence, we postulate the following hypotheses:

1. Gentle application of the washing liquid to the filter cake surface using capillaries as dosing units results in higher washing efficiency than nozzle-based units.
2. The usage of an efficient dosing unit with the minimal wash ratio during washing can eliminate the need for an additional drying step, while achieving the targeted residual solid content and PSD maintenance.

To verify these hypotheses, we investigated various dosage units for the application of washing liquid systematically with respect to their washing efficiency for particles in a size range of 355–560 µm in the first washing step based on wash curve analysis. In addition, the influence of the wash ratio in the second washing step on CQAs including residual moisture and PSD maintenance was evaluated utilizing the most effective dosage unit in the first washing step.

2. Materials and methods

2.1. System investigated

In this study, the L-alanine/water substance system was employed as a cost-effective model substance system exhibiting physicochemical properties comparable to those of APIs. Data regarding solubility, crystal morphology, filterability, agglomeration tendency, and cooling crystallization behavior have been widely reported in literature [19–22]. Most previous studies on CVSF characterization are based on the L-alanine/water substance system, thereby ensuring consistency and comparability of the results [14,16,17,23,24]. Beyond its suitability as a model compound, L-alanine is considered biologically safe, as it is an endogenously produced amino acid and an essential constituent of

protein structures [25]. Amino acids play a key role in pharmaceutical and nutritional industries and are therefore produced in large quantities, with worldwide demand continuing to grow [25–27]. For the experimental work, L-alanine (Evonik Industries AG, 99.7% purity, $\rho_{solid} = 1420\ kg\ m^{-3}$) was recrystallized from aqueous solution and classified by sieving to obtain the desired particle size fraction of 355–560 µm (bipyramidal, $\varepsilon = 45.1\%$). Ultrapure water (Merck KgaA, Milli-Q Advantage A10, 0.05 µS cm^{-1}) was utilized as solvent for the preparation of L-alanine solutions at 20 °C in accordance with the solubility curve of the L-alanine/water system described by Eq. (2) [28].

$$c^{*}_{Ala}\left[g_{Ala} \bullet g^{-1}_{sol}\right] = 0.11238 \bullet \exp\left(9.0849 \bullet 10^{-3} \bullet \vartheta\left[^{\circ}C\right]\right) \quad (2)$$

Absolute ethanol (VWR Chemicals) was used as the antisolvent for the L-alanine/water substance system. Accordingly, an ethanol/water mixture (4,1, v/v) was employed as washing liquid in the first washing step, whereas pure ethanol was used in the second washing step.

2.2. Experimental setup and procedures

The experimental setup of the CVSF including the periphery used in this study is depicted in Fig. 1. A detailed description of the experimental setup can be found in our previous publication [29]. Additionally, the screw, including its characteristic design parameters, is presented in Fig. 2.

The experimental investigation of the two-stage washing process was based on the CVSF configuration providing filtration and two-stage washing (FWW). The design, input, and operating parameters are given in Table 1. The traceability of the solid phase in the CVSF for the operating point established screw design used in this work has been proven in a previous study [14].

In this work, the washing liquid volume flow rates in both washing steps were varied in order to evaluate the washing efficiency and product quality depending on the respective wash ratio. The washing liquid was applied via four different stainless steel dosing units shown in Fig. 3.

All tested wash ratios in the respective washing steps were evaluated based on duplicate experiments with triplicate sampling. To assess PSD maintenance during continuous particle isolation within the CVSF, the

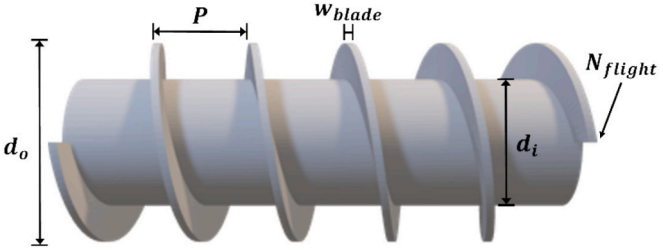

Fig. 2. Schematic picture of the screw made of polytetrafluoroethylene (PTFE), including the characteristic screw design parameters as given in Table 1.

Table 1
Overview of constant design, input, and process parameters for the experiments conducted.

Parameters		Value
Design	Module inner diameter $d_{i,module}$	25.2 mm
	Screw length L_{screw}	240 mm
	Inner screw diameter d_i	16 mm
	Outer screw diameter d_o	25 mm
	Pitch distance P	12 mm
	Screw blade width w_{blade}	1 mm
	Flight number N_{flight}	1
	Pore size of filter medium	40–100 µm
Input	Suspension volume flow rate Q_{susp}	20 mL min^{-1}
	Solid loading w_{solid}	6 wt.-%
	Particle shape	Bipyramidal
	Particle size fraction	355–560 µm
	Suspension temperature ϑ_{susp}	20 °C
	Rotational screw speed n_{screw}	1 rpm
	Washing liquid 1	Ethanol/water mixture (4:1 v/v)
	Washing liquid 2	Absolute ethanol
Process	Filling degree α	50%
	Temperature increase preheater ΔT	3 K
	Maximum pressure drop Δp	400 mbar
	Vacuum pump frequency f_{VP}	26 Hz

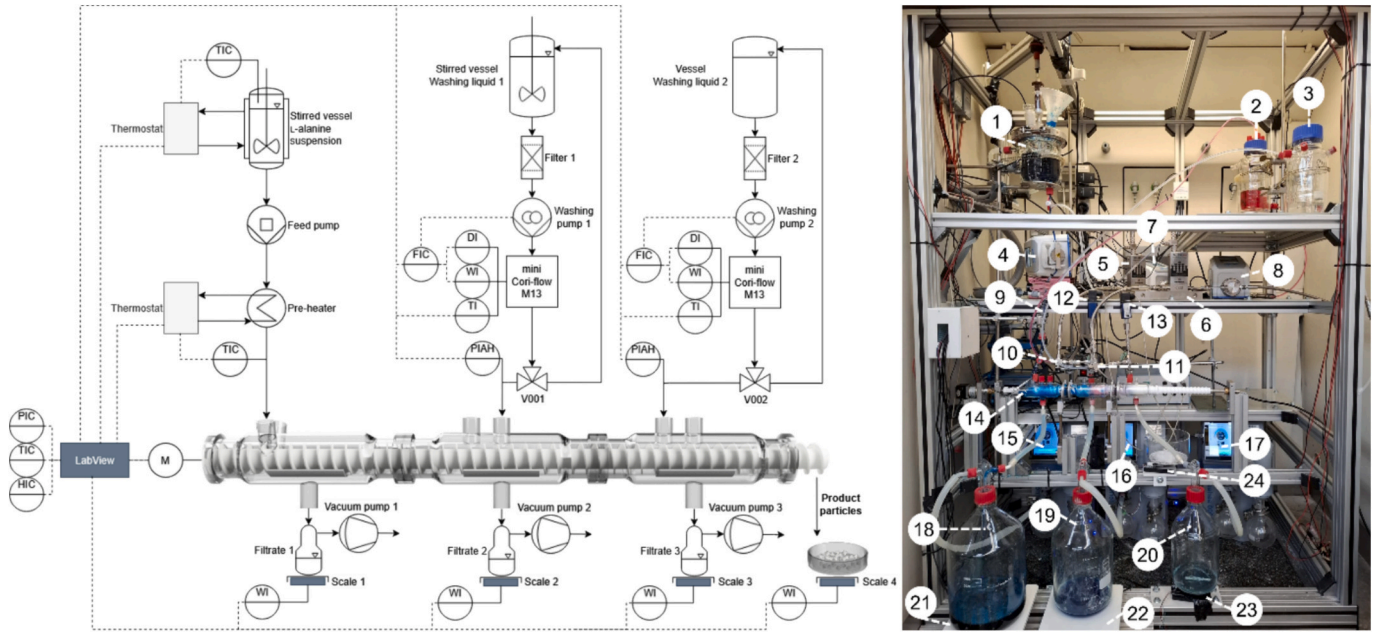

Fig. 1. Experimental setup of the CVSF with one filtration and two washing modules with its periphery and control strategy. (Left) schematic representation, (Right) picture with (1) feed vessel, (2)/(3) vessel for washing liquid 1 and 2, (4) feed pump, (5)/(6) coriolis flow meter for washing liquids 1 and 2, (7)/(8) washing pumps 1 and 2, (9) preheater, (10)/(11) three-way valves V001 and V002, (12)/(13) pressure sensors 1 and 2, (14) CVSF itself, (15)–(17) vacuum pumps 1–3, (18)–(20) filtrates 1–3, (21)–(24) scales 1–4.

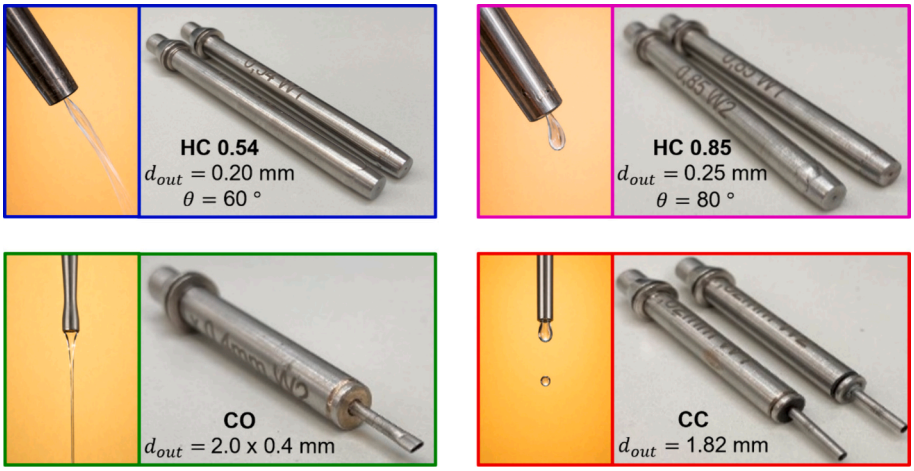

Fig. 3. Dosing units tested in this study for washing liquid application with their geometries and qualitatively characteristic liquid flow pattern at an exemplary washing volume liquid flow rate in the first washing step of 15 mL min^{-1}. (a) hollow cone nozzle with an outlet diameter d_{out} of 0.20 mm and a spray angle θ of 60° (Lechler GmbH, 220.054, HC 0.54), used as standard dosing unit for washing liquid application in our previous publications [14,24] (b) hollow cone nozzle with a larger outlet diameter d_{out} of 0.25 mm and spray angle θ of 80° (Lechler GmbH, 220.085, HC 0.85) (c) capillary with an oval outlet geometry (d_{out} = 2.0 × 0.4 mm, CO) (d) capillary with a circular outlet geometry (d_{out} = 1.82 mm, CC).

PSD of the feed particles was measured twice prior to entering the CVSF, assuming that all feed particles originated from the same statistical population. The PSD of the particles leaving the apparatus at the outlet was determined twice at each operating point of the respective washing process in each experiment. The underlying data of this study are available via the TUDOdata research repository in our data publication [30]. The optimization of the two-stage washing procedure within the CVSF is structured as follows:

1) Identifying most efficient dosing unit and optimal operating point of the first washing step based on wash curves.

2) Optimizing the second washing step based on the optimized first washing step regarding residual moisture and PSD maintenance.

2.2.1. Optimization of the first washing step

For the optimization of the first washing step, the evaluation of the purification performance of the product particles is fundamental. Therefore, coloring experiments were conducted in order to assess the purification performance of the two-stage washing process within the CVSF qualitatively and quantitatively. Hence, the dye brilliant blue (BB, Carl Roth GmbH & Co. KG) was added to the mother liquor of the particle suspension at a concentration of 1 mg mL^{-1} and the red dye chromotrope (CH, Carl Roth GmbH & Co. KG) was added to the first washing liquid at a concentration of 0.04 mg mL^{-1} to assess the two-stage washing process qualitatively based on visible color transitions.

In addition, brilliant blue BB acts as an artificial impurity for a quantitative evaluation. A detailed description of the experimental procedure for the determination of the BB mass loading ratio after each process step can be found in our previous study [14] and is summarized here briefly. The BB mass loading ratio $X^*_{BB,i}$ with respect to the product particles is used as a quantitative measure. It is defined as the ratio of BB mass loading after a specific process step i $X_{BB,i}$ normalized by the initial BB mass loading in the feed suspension $X_{BB,0}$ (Eq. (3)). The BB mass loading after process step i $X_{BB,i}$ is given by the ratio of the BB mass $m_{BB,i}$ to solid mass $m_{solid,i}$ in a sample taken after process step i (Eq. (4)).

$$X^*_{BB,i} = \frac{X_{BB,i}}{X_{BB,0}} \tag{3}$$

$$X_{BB,i} = \frac{m_{BB,i}}{m_{solid,Ala,i}} \tag{4}$$

In the pharmaceutical industry, the threshold at which impurities must be reported is at 300 ppm for API dosages over 2 g d^{-1} [31]. Nevertheless, in this study, an ambitious final BB mass loading after the first washing step of about 5 ppm was targeted for final product purity. Based on a $X_{BB,0}$ of approximately 18,000 ppm, a final BB mass loading of 5 ppm corresponds to a BB mass loading ratio of 0.03% to be ensured already after the first washing step in order to guarantee sufficiently high product purity.

In the context of optimizing the first washing step, wash curves were generated for each dosing unit (Fig. 3) by determining the BB mass loading ratio after the first washing step for multiple wash ratios, as schematically depicted in Fig. 4.

Therefore, a wash curve was determined in each experiment by

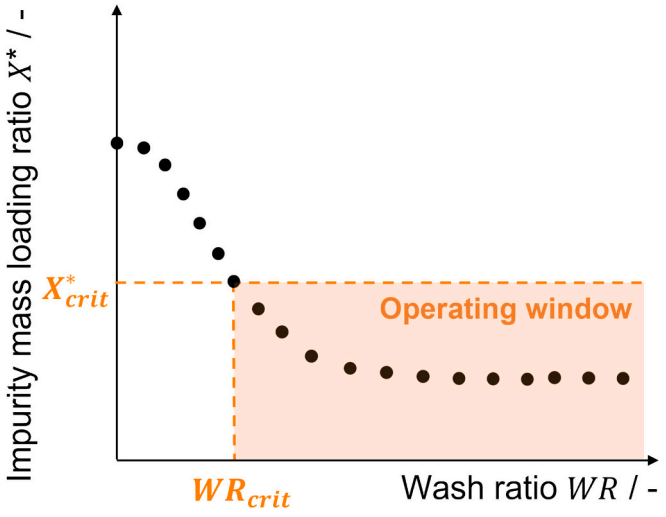

Fig. 4. Schematic wash curve, which relates the impurity mass loading ratio X^* to the wash ratio WR. The targeted critical impurity mass loading ratio is denoted by X^*_{crit} and the minimum required wash ratio in order to guarantee sufficiently high product purification by WR_{crit}. The operating window for the washing process is defined by X^*_{crit} and WR_{crit} and indicated by the orange area in the diagram.

successive reduction of washing liquid volume flow rate or the wash ratio, respectively. In order to ensure valid sampling of filter cake washed at a specific wash ratio at the CVSF outlet, the 1.5-fold measured mean particle residence time until particle discharge at CVSF outlet was awaited after setting a new wash ratio in the first washing step [14]. For the generation of the wash curves for the first washing step, the FWW configuration was realized, while the second washing module was deactivated to guarantee representative fluid dynamics in the first washing module for integrated CVSF operation. Based on the defined critical BB mass loading ratio $X^*_{BB,crit}$ of 0.03%, the minimum wash ratio WR_{crit} or washing liquid consumption was determined from the respective washing curve for each tested dosing unit. Ultimately, the most efficient dosing unit was identified by comparing the minimum required wash ratios in the first washing step of the respective dosing units.

2.2.2. Optimization of the second washing step

The second washing step focuses on the CQAs residual moisture of the particles and PSD maintenance. The residual moisture ϕ_{RM} is calculated according to Eq. (5) and is defined as the relative ratio of the liquid mass m_{liquid} to the total mass, consisting of liquid and solid m_{solid} masses.

$$\phi_{RM} = \frac{m_{liquid}}{m_{liquid} + m_{solid}} \bullet 100\% \tag{5}$$

The PSD maintenance as essential requirement for continuous particle isolation is evaluated by the comparison of the characteristic values of the PSD ($d_{50,3}, d_{90-10,3}$) and the agglomeration degree (Eq. (6)) of the feed particles prior to entering the CVSF ($Ag_{3,in}$) with the respective values leaving the apparatus at CVSF outlet ($Ag_{3,out}$). Here, the objective is to ensure that the agglomeration degree of the particles after being processed within the CVSF was less than or equal to that of the feed particles. The PSD measurements were conducted via offline dynamic image analysis using a QICPIC sensor (Sympatec GmbH) equipped with a LIXELL wet dispersion module with a 2 mm flow cell gap width at ambient conditions. The procedures for the experimental determination of the residual moisture and PSD can be found in our previous work [14].

$$Ag_3 = \frac{V_{non-single\ particles}}{V_{non-single\ particles} + V_{single\ particles}} \bullet 100\% \tag{6}$$

After successful displacement washing of the impurity in the first washing step, the washing liquid from the first washing step (ethanol/water 4:1 v/v) remains in the pore system of the filter cake. During the transport of the filter cake to the second washing step, the ethanol preferentially evaporates from the pore liquid, resulting in an increased water content in the pore liquid. The remaining water in the filter cake can subsequently cause partial redissolution of the particles. If a drying step is added directly after the first washing step, L-alanine redissolved in the pore liquid will recrystallize during water evaporation. This recrystallization may lead to changes in the PSD by increasing the agglomeration degree. This phenomenon is demonstrated in our previous publication [14]. Consequently, a second washing step is essential to displace the residual water from the pore system of the filter cake using pure ethanol, thereby minimizing the influence of the two-stage washing process on the PSD and providing the potential to achieve a low residual moisture of less than 1% without the need for an additional drying step.

However, the achievable residual moisture after the second washing step depends on the particle and filter cake properties [32], the residence time between application of the second washing liquid and particle discharge at the CVSF outlet [29], as well as the applied washing liquid amount. Optimizing the amount of washing liquid in the second washing step avoids unnecessary excess of washing liquid, which would otherwise lead to an undesired increase in residual moisture at the CVSF outlet. By determining the minimum required wash ratio to ensure complete displacement of residual water by ethanol, the target residual moisture may be achieved while eliminating the need for an additional drying step.

3. Results

3.1. Optimizing first washing step

Fig. 5 shows the wash curves for the different dosing units (Fig. 3). All experimentally determined wash curves exhibit the characteristic behavior of wash curves (Fig. 4), indicating an asymptotic convergence of product purification or purity with increasing wash ratio [33]. This behavior can be attributed to a fraction of impurities that is strongly adsorbed onto the particle surface as well as to pores or dead zones within the filter cake that are inaccessible to the washing liquid and therefore cannot be removed, regardless of the applied wash ratio [34,35].

The washing efficiency strongly depends on the dosing unit employed. For the hollow cone nozzle HC 0.54 used as standard dosing unit (blue squares), the wash curve reveals that the washing liquid consumption can be reduced by approximately 50% compared to the standard operating point, while still achieving the required particle purity. This corresponds to a reduction in wash ratio from 20.4($Q_{WL,1}$ = 15 mL min^{-1}) to 9.5 ($Q_{WL,1}$ = 7 mL min^{-1}). In contrast, the hollow cone nozzle with the larger outlet geometry (HC 0.85, pink diamonds) exhibited unstable operating behavior. This instability was reflected by inconsistent discharge of the washing liquid in the form of droplets or a lamella, as also qualitatively illustrated in Fig. 3. Correspondingly, the respective wash curve in Fig. 5 displays pronounced fluctuations and comparatively large error bars. Consequently, starting at the standard operating point in the first washing step ($Q_{WL,1}$ = 15 mL min^{-1}), no lower wash ratio was identified to reliably ensure the target particle purification. The wash curve associated to the capillary with oval outlet geometry (CO, green triangles) shows a reduction in washing liquid consumption of minimum 66%, decreasing from the standard wash ratio

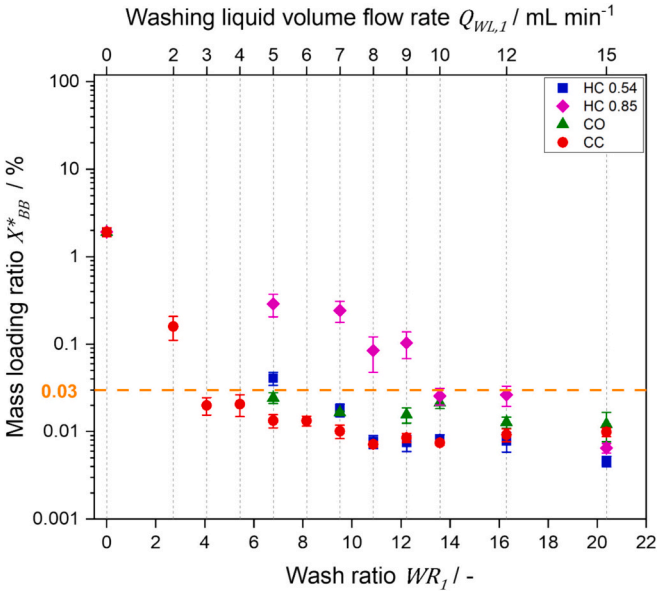

Fig. 5. Experimentally determined wash curves for all tested dosing units (Fig. 3) with the constant parameters given in Table 1. The mass loading ratio X^*_{BB} is plotted against the wash ratio WR (lower x-axis). The corresponding washing liquid flow rates $Q_{WL,1}$ are shown on the upper x-axis and marked by vertical grey dotted lines. The target purification $X^*_{BB,crit}$ of 0.03% corresponding to a target purity $X_{BB,crit}$ of 5 ppm is indicated by the orange dashed line. The underlying data are available in our data publication [30].

of 20.4 ($Q_{WL,1}$ = 15 mL min^{-1}) to a critical wash ratio of about 6.8 ($Q_{WL,1}$ = 5 mL min^{-1}). The highest washing efficiency was achieved using the capillary with circular outlet geometry (CC, red circles). The related wash curve indicates that the required particle purification can be maintained down to a wash ratio of approximately 4.1 ($Q_{WL,1}$ = 3 mL min^{-1}), corresponding to a reduction in washing liquid consumption of about 80%.

A possible explanation for the observed differences in wash curves and washing efficiencies among the dosing units lies in the varying washing liquid velocities hitting the filter cake surface at identical volumetric flow rates. These velocity differences arise from the specific outlet geometries of the respective dosing units. Previous studies have shown that the application of washing liquid at high velocity on the filter cake surface, for example through nozzle-based dosing systems, can adversely affect washing performance [36,37]. The kinetic energy of the washing liquid hitting the filter cake surface may induce localized turbulence or partial resuspension of particles at the cake surface. As a result, impurities initially contained within the pore structure can prematurely mix with the washing liquid, leading to contamination of the washing liquid before effective displacement washing occurs. This correlation between the washing liquid velocity contacting the filter cake surface and the resulting washing efficiency is also reflected in Fig. 6, presenting the washing liquid velocity for different washing liquid volume flow rates or wash ratios depending on the dosing unit employed.

As shown in Fig. 6, the washing liquid velocities generated by the hollow cone nozzles HC 0.54 and HC 0.85 are significantly higher over the investigated wash ratio range than those achieved with the capillaries CO and CC. The lower velocities associated with the capillary-based dosing units result in a gentler application of the washing liquid onto the filter cake surface, thereby enabling higher washing efficiencies. However, not only the velocity at which the washing liquid is applied to the filter cake is decisive for achieving high washing efficiency, but also a consistent discharge of the washing liquid from the dosing unit in the form of droplets or lamellae, ensuring that the entire filter cake surface is reached by the washing liquid. As shown in Fig. 6, HC 0.85 exhibits a lower discharge velocity of washing liquid at a specific wash ratio compared to HC 0.54. Nevertheless, the corresponding wash curves in Fig. 5 indicate that HC 0.54 achieves a higher washing efficiency. This can be attributed to the previously described inconsistent washing liquid discharge of HC 0.85.

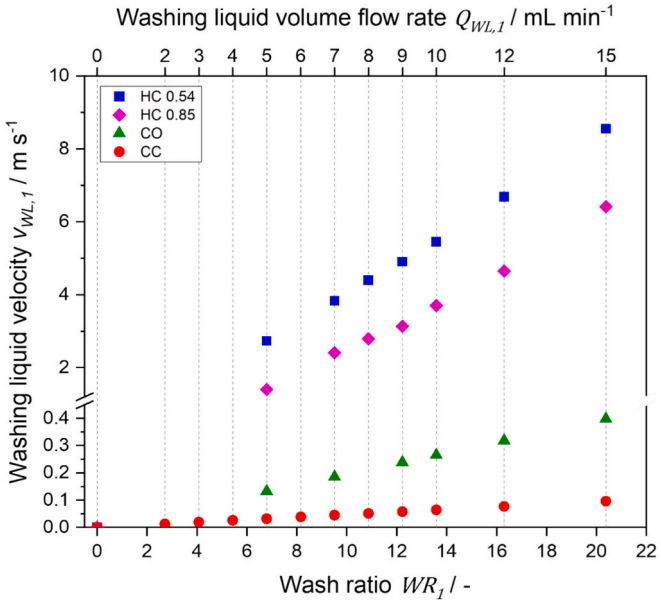

Fig. 6. Calculated washing liquid velocity $v_{WL,1}$ (y-axis) for all tested dosing units against the wash ratio WR_1 (lower x-axis) or the washing liquid volume flow rate $Q_{WL,1}$ (upper x-axis) in the first washing step. The washing liquid volume flow rates $Q_{WL,1}$ corresponding to the respective wash ratios WR_1 are marked by grey dotted lines. The blue squares represent the washing liquid velocity employing the HC 0.54 dosing unit, the pink diamonds the washing liquid velocity using the HC 0.85, the green triangles the washing liquid velocity using the CO, and the red circles the washing liquid velocity utilizing the CC (Fig. 3). The underlying calculations are available in our data publication [30]. (For interpretation of the references to color in this figure legend, the reader is referred to the web version of this article.)

3.2. Optimizing second washing step

The second washing step of the two-stage washing process within the CVSF was optimized based on the optimal operating conditions (CC, $Q_{WL,1}$ = 3 mL min^{-1}, WR_1 = 4.1) determined in the preceding first washing step (section 3.1). The CC dosing unit was therefore applied in the second washing step. The optimization of the second washing step aimed for PSD maintenance while ensuring the targeted residual moisture of less than 1% within a defined wash ratio range. Since the target product purity had already been achieved by the first washing step, further purification was not addressed in the second washing step. The results concerning PSD maintenance (agglomeration degree) and residual moisture as a function of wash ratio in the second washing step are presented in Fig. 7.

Fig. 7 reveals that the residual moisture of the particles after the second washing step decreases with decreasing wash ratio down to 4.1, reaching a minimum at this value, and increases upon further reduction of the wash ratio. The residual moisture, particularly the minimum across the examined wash ratio range in the second washing step, reflects the efficiency of displacement washing in this step. At high wash ratios ($WR_2 \geq 11$), the applied excess of washing liquid (ethanol) results in complete displacement of residual water from the filter cake pore system originating from the first washing step. However, the excess

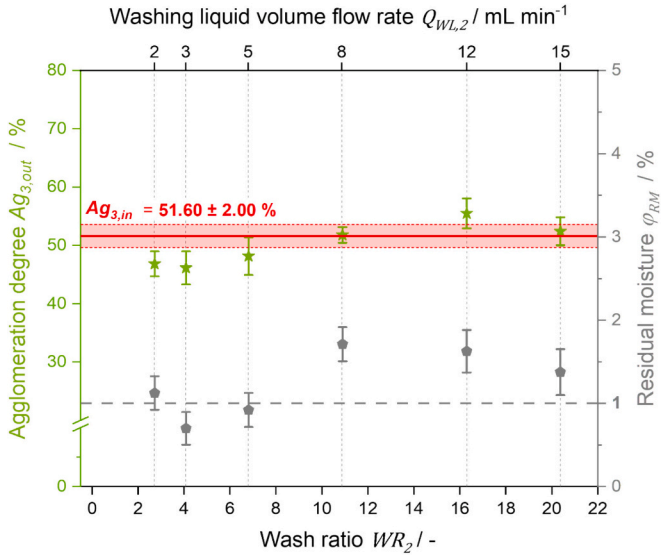

Fig. 7. Experimental results regarding the agglomeration degree of the particles leaving the apparatus at the CVSF outlet $Ag_{3,out}$ (green star, left y-axis) and the residual moisture of the particles ϕ_{RM} (grey pentagon, right y-axis) as a function of the wash ratio WR_2 (lower x-axis) or the corresponding washing liquid volume flow rate $Q_{WL,2}$ (upper x-axis) in the second washing step, indicated by vertical dotted grey lines. The horizontal solid red line marks the reference agglomeration degree of the particles prior to entering the CVSF $Ag_{3,in}$ and the upper and lower horizontal dashed red line the respective standard deviation. Moreover, the horizontal dashed grey line indicates the targeted residual moisture of 1%. The underlying calculations are available in our data publication [30]. (For interpretation of the references to color in this figure legend, the reader is referred to the web version of this article.)

ethanol cannot be sufficiently removed by filtration, deliquoring, and evaporation from the filter cake during the residence time in the second washing module, preventing residual moisture results below 1%. The minimum residual moisture observed at a wash ratio of 4.1 represents an optimal compromise between efficient displacement of pore water and a minimum amount of ethanol that must be removed until filter cake discharge at the CVSF outlet. Here, the target residual moisture is ensured without the need for an additional drying step. At a further reduced wash ratio ($WR_2 = 2.7$), the applied amount of washing liquid is insufficient to completely displace water from the filter cake pore system, resulting in higher residual moisture. Water is more difficult to remove from porous media under vacuum conditions than ethanol due to its higher surface tension and stronger wetting of hydrophilic particle surfaces, leading to significantly higher capillary pressures [38,39], as well as its lower vapor pressure at constant temperature [40–42]. Consequently, the higher water content in the pore liquid at a wash ratio of 2.7 results in higher residual moisture at the CVSF outlet compared to a wash ratio of 4.1.

Consistent with the residual moisture trends, Fig. 7 further indicates that the agglomeration degree after CVSF processing ($Ag_{3,out}$) decreases with decreasing wash ratio. This suggests that residual moisture influences the resulting agglomeration degree, as increased moisture within the filter cake promotes interparticle adhesion and the formation of aggregates or agglomerates. However, it should be noted that PSD measurements using dynamic image analysis cannot differentiate between agglomerates and loose aggregates. At the wash ratio of 4.1 corresponding to minimum residual moisture, the agglomeration degree after CVSF processing ($Ag_{3,out}$) is lowest and lower than that of the feed particles ($Ag_{3,in}$), thereby fulfilling the requirement for PSD maintenance.

3.3. Comparison of established and optimized two-stage washing within the CVSF

To emphasize the benefits of an optimized two-stage washing process (sections 3.1 and 3.2) versus the established washing process based on the experimental setup described in section 2.2, both processes are compared regarding washing efficiency and product quality qualitatively and quantitatively. The respective washing conditions are listed in Table 2.

Fig. 8 provides a qualitative, image-based comparison of both washing concepts. The established washing process (a) exhibits a markedly sharper color transition from blue to red in the first washing step (FW) compared to the optimized washing process (b). This distinct color transition results from the relatively high wash ratio or washing liquid volume flow rate applied in the first washing step of the established process, resulting in a significantly higher product purity compared to the optimized washing process. In contrast, after application of the washing liquid in the first washing step of the optimized process, no distinct color transition from blue to red is observed. Instead, the filter cake appears violet, which, in accordance with Fig. 8, indicates a higher but sufficiently low residual BB mass loading or product purity, respectively. Although the primary focus of the second washing step (FWW) is on PSD maintenance and the achievement of the targeted final residual moisture of less than 1%, the qualitative observations demonstrate that the second washing step also contributes to further purification with respect to the residual BB mass loading. Consequently, the color transition from violet to colorless observed during the second washing step (FWW) of the optimized washing process indicates that, despite the visually lower impurity removal achieved after the first washing step, the same final product purity with respect to the artificial impurity BB as in the established washing process seems to be ensured.

Table 2
Overview of operating conditions of the established and optimized washing process.

Parameters	Established washing	Optimized washing
Dosing unit	HC 0.54	CC
$Q_{WL,1}$ [mL min^{-1}]	15	3
WR_1 [−]	20.4	4.1
$Q_{WL,2}$ [mL min^{-1}]	15	3
WR_2 [−]	20.4	4.1

In both washing processes, all the other parameters stay constant according to Table 1. $Q_{WL,1}$ and $Q_{WL,2}$ denote the washing liquid volume flow rates in the first and second washing step, respectively, and WR_1 and WR_2 the corresponding wash ratios.

Fig. 9 depicts the comparison between established (clear bars) and optimized (hatched bars) two-stage washing concept in terms of impurity removal (left blue bars) and residual moisture (right grey bars) after each process step, meaning filtration (F), filtration and first washing (FW) and filtration and two-stage washing (FWW).

Both washing concepts exhibit similar results after the filtration step (F) in terms of BB mass loading and residual moisture due to identical operating conditions during the filtration step. Differences in the BB mass loading ratio or BB mass loading after the filtration step are attributed to inhomogeneities in the BB mass loading of the sampled filter cake. After the first washing step (FW), the targeted purification of $X^*_{BB} < 0.03\%$ is ensured in both concepts, whereby the optimized washing process requires 80% less washing liquid compared to the established washing process. Due to the significantly higher washing liquid consumption, the established washing process achieves a higher product purity after the first washing step with a residual BB mass loading X_{BB} of 0.8 ppm than the optimized washing process (3.9 ppm). The residual moisture of the particles after the first washing step is approximately 10% for both washing concepts. By optimizing the second washing step (FWW), the same purification performance as that of the established washing process was achieved, resulting in a residual BB mass loading of 0.6 ppm, while reducing washing liquid consumption by 80%. For both washing concepts, further product purification below approximately 0.5 ppm cannot be achieved by washing due to limiting physical effects, namely strong adsorption of BB onto the particle surface as well as inaccessible pores and dead zones within the filter cake [33–35]. Finally, the optimized two-stage washing process ensured the targeted residual moisture of less than 1% without the need for an additional drying step, as would be required for the established washing process.

Fig. 10 shows the results of the PSD at the outlet of the CVSF after two-stage washing (FWW) for the established washing concept (left) and the optimized washing concept (right). The red diamonds denote the inlet PSD (PSD_{in}) and the green squares to the outlet PSD (PSD_{out}), which should equal to ensure PSD maintenance. For the established washing process (left) this is not ensured, as PSD_{in} and PSD_{out} exhibit a distinct deviation. This deviation is attributed to an increased agglomeration degree $Ag_{3,out}$, which is also reflected by an increased mean particle size $d_{50,3}$ and a broader PSD $d_{90-10,3}$. The enhanced agglomeration and thus the deviation between PSD_{in} and PSD_{out} is likely caused by the higher residual moisture after the two-stage washing process ($\phi_{RM} = 1.9\%$, Fig. 9) as well as by enhanced redissolution effects resulting from the excess of washing liquid applied in both washing steps during this concept, as discussed in section 2.2.2. In contrast, PSD maintenance is observed for the optimized washing process (right). Accordingly, the mean particle sizes of PSD_{in} and PSD_{out} are nearly equal, and PSD_{out} exhibits only a slightly broader PSD, but with lower agglomeration degree $Ag_{3,out}$. Overall, the optimized two-stage washing process enables improved product quality compared to the established washing process by maintaining the PSD, which is essential for continuous particle isolation.

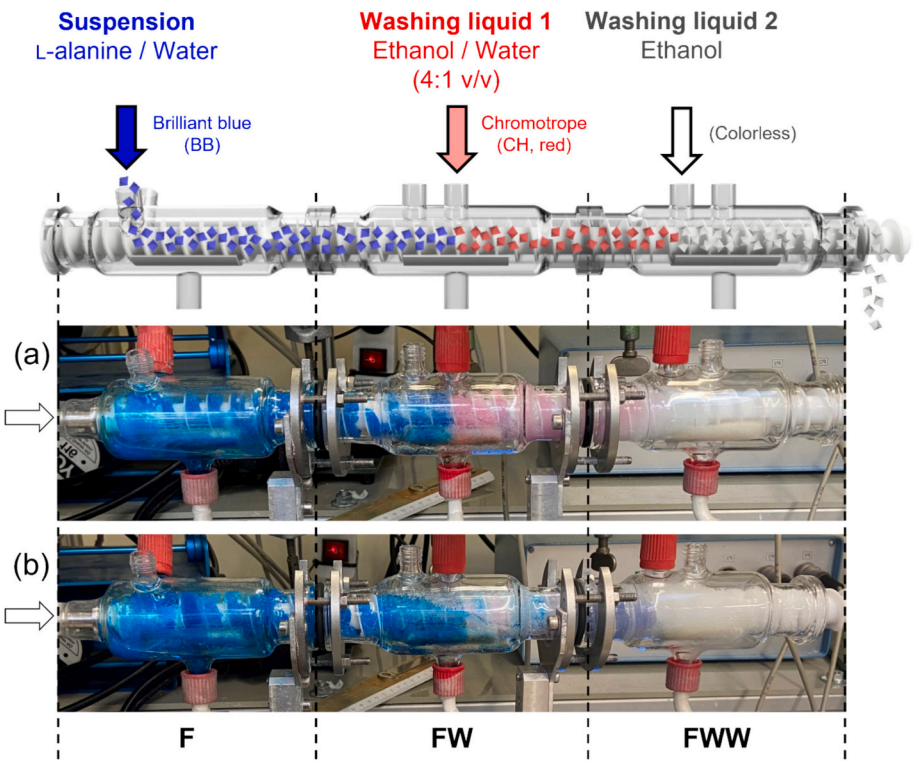

Fig. 8. Visual comparison of the established (a) and optimized (b) two-stage washing processes together with a schematic of the experimental setup in the FWW configuration, including the suspension feed and both washing liquid streams into the CVSF at the top. The underlying calculations are available in our data publication [30].

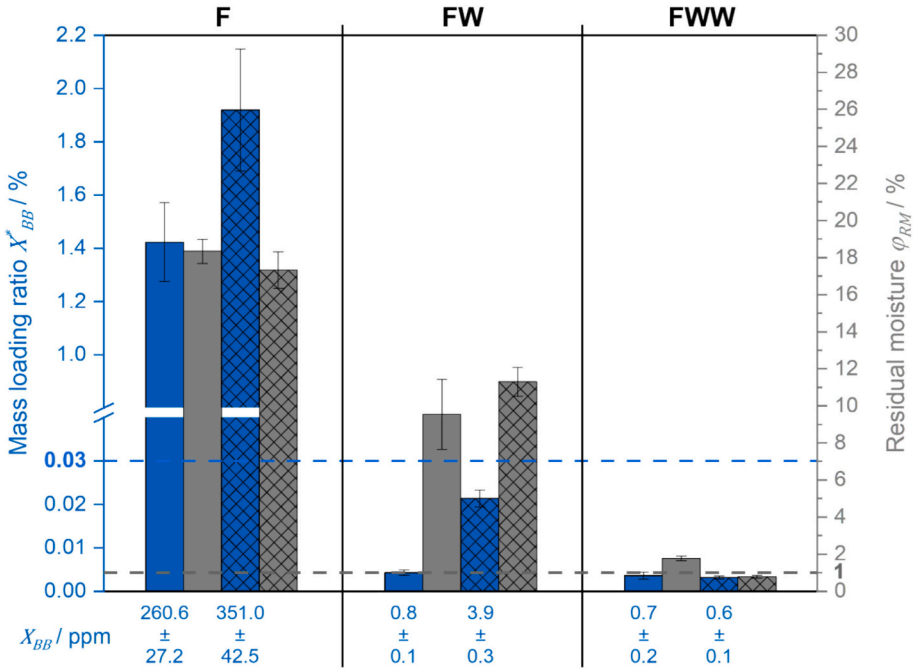

Fig. 9. Results regarding impurity removal, namely the mass loading ratio X^*_{BB} (blue bars, left y-axis) and mass loading X_{BB} (x-axis), as well as the residual moisture ϕ_{RM} (grey bars, right y-axis) for the established (clear bars) and optimized (hatched bars) two-stage washing process. (Left) after filtration (F), (middle) after filtration and first washing step (FW), and (right) after filtration and two-stage washing (FWW). The blue horizontal dashed line marks the targeted X^*_{BB} of 0.03% and the grey horizontal dashed line indicates the aimed ϕ_{RM} of 1%. The underlying calculations are available in our data publication [30]. (For interpretation of the references to color in this figure legend, the reader is referred to the web version of this article.)

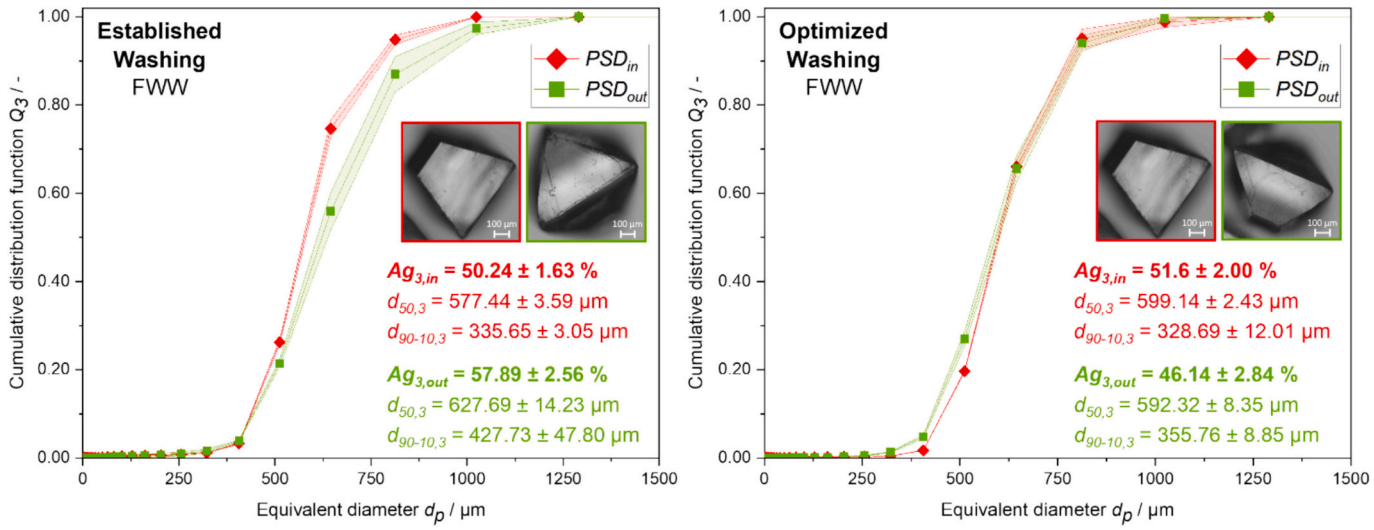

Fig. 10. Comparison of the PSD of the feed particles entering the CVSF (PSD_{in}, red diamonds) and the particles discharged at the CVSF outlet (PSD_{out}, green squares) after two-stage washing (FWW). The cumulative distribution function Q_3 is plotted as a function of the equivalent particle diameter d_p. The PSDs are further characterized by the agglomeration degree Ag_3, the mean particle size $d_{50,3}$, and the PSD width $d_{90-10,3}$. Representative microscope images of particles corresponding to each PSD are shown using the respective frame colors. The left-hand diagram refers to the established washing process, while the right-hand diagram shows the PSD results concerning the optimized washing process. The underlying calculations are available in our data publication [30]. (For interpretation of the references to color in this figure legend, the reader is referred to the web version of this article.)

4. Conclusion

This study focused on optimizing the two-stage washing process within the CVSF for product particles in the size range of 355–560 µm, with the primary objective of minimizing washing liquid consumption while fulfilling the requirements for continuous particle isolation. These requirements included a residual impurity loading below 5 ppm, a final residual moisture below 1%, and particle size distribution (PSD) maintenance throughout the isolation process.

In a first step, the first washing step was optimized with respect to washing efficiency, defined as the washing liquid consumption required to achieve a specific product purity. Based on experimentally determined wash curves, the influence of four different washing liquid dosing units and wash ratios on washing efficiency was evaluated. The results demonstrated that capillaries provide significantly higher washing efficiency than hollow cone nozzles due to the gentler application of washing liquid to the filter cake surface. In particular, the capillary with circular outlet geometry enabled a reduction in washing liquid consumption by 80%, corresponding to a wash ratio of 4, compared to the established operating point using a hollow cone nozzle at a wash ratio of 20, while simultaneously ensuring the targeted product purity with a residual impurity loading below 5 ppm.

Based on the optimized first washing step, the second washing step was subsequently optimized using a capillary with circular outlet geometry as the dosing unit in both steps. The optimization focused on achieving a residual moisture content below 1% and maintaining the PSD. The non-optimized washing process did not achieve the targeted residual moisture below 1% and could not ensure PSD maintenance after filtration and two-stage washing, thereby requiring an additional drying step. In contrast, optimization of the two-stage washing process within the CVSF fulfills all requirements for continuous particle isolation while reducing washing liquid consumption by 80%. This decreases the required amounts from 20 L of ethanol and 2.5 L of water to approximately 4 L of ethanol and 0.5 L of water per kilogram of processed solid material, corresponding to annual savings of about 11,500 L of ethanol and 1,300 L of water. Overall, this study demonstrates the significant ecological and economic potential of optimizing the two-stage washing process within the CVSF.

Future research should address the transferability of the optimized two-stage washing process to various particle sizes or shapes, screw designs, rotational screw speeds, and solids throughputs within the CVSF. For increased production capacities, numbering-up of multiple CVSF units seems more reasonable than scaling-up a single CVSF unit by increasing its diameter. The small-scale design of the CVSF ensures a uniform distribution of the washing liquid across the filter cake using a capillary dosing unit with a circular outlet geometry. With increasing CVSF diameter, maintaining a homogeneous washing liquid distribution across the entire filter cake surface area will become increasingly challenging, potentially leading to reduced washing efficiency. In contrast, numbering-up will preserve the geometric and hydrodynamic conditions of the validated small-scale system, including the local washing liquid velocity and distribution characteristics, thereby facilitating reliable transfer of washing efficiency to higher throughput levels. Such investigations are essential to enable predictive determination of optimal operating conditions for a specific impurity under varying process conditions, thereby further enhancing the flexibility and robustness of continuous particle isolation utilizing the CVSF.

Declaration of competing interest

The authors declare the following financial interests/personal relationships which may be considered as potential competing interests:

Kerstin Wohlgemuth reports financial support was provided by German Research Foundation. Kerstin Wohlgemuth has patent #WO2021148108A1 pending to Technische Universitaet Dortmund. Given her role as reviewer, Kerstin Wohlgemuth had no involvement in the peer review of this article and had no access to information regarding its peer review. Full responsibility for the editorial process for this article was delegated to another journal editor. If there are other authors, they declare that they have no known competing financial interests or personal relationships that could have appeared to influence the work reported in this paper. If there are other authors, they declare that they have no known competing financial interests or personal relationships that could have appeared to influence the work reported in this paper.

Acknowledgement

Our research receives funding by the German Research Foundation (Deutsche Forschungsgemeinschaft – DFG) in the framework of the Priority Programme PP 2364 – Project No. 504676854.

The authors express their special thanks to Tobias Pape and Daniela Schölzel for their technical support during the experiments.

Data availability

The data supporting the findings of this study are provided in accordance with the FAIR principles via the data repository TUDOdata at the following DOI: https://doi.org/10.17877/TUDODATA-2026-JVFCSI

References

[1] J. Orehek, D. Teslić, B. Likozar, Continuous crystallization processes in pharmaceutical manufacturing: a review, Org. Process. Res. Dev. 25 (2021) 16–42, https://doi.org/10.1021/acs.oprd.0c00398.
[2] D. Zhang, S. Xu, S. Du, J. Wang, J. Gong, Progress of pharmaceutical continuous crystallization, Engineering 3 (2017) 354–364, https://doi.org/10.1016/j.eng.2017.03.023.
[3] M. Baumann, T.S. Moody, M. Smyth, S. Wharry, A perspective on continuous flow chemistry in the pharmaceutical industry, Org. Process. Res. Dev. 24 (2020) 1802–1813, https://doi.org/10.1021/acs.oprd.9b00524.
[4] A. Hyer, D. Gregory, K. Kay, Q. Le, J. Turnage, F. Gupton, J.K. Ferri, Continuous manufacturing of active pharmaceutical ingredients: current trends and perspectives, Adv. Synth. Catal. 366 (2024) 357–389, https://doi.org/10.1002/adsc.202301137.
[5] A. Kumar, K.V. Gernaey, T. de Beer, I. Nopens, Model-based analysis of high shear wet granulation from batch to continuous processes in pharmaceutical production - a critical review, Eur. J. Pharm. Biopharm. 85 (2013) 814–832, https://doi.org/10.1016/j.ejpb.2013.09.013.
[6] G. Allison, Y.T. Cain, C. Cooney, T. Garcia, T.G. Bizjak, O. Holte, N. Jagota, B. Komas, E. Korakianiti, D. Kourti, R. Madurawe, E. Morefield, F. Montgomery, M. Nasr, W. Randolph, J.-L. Robert, D. Rudd, D. Zezza, Regulatory and quality considerations for continuous manufacturing May 20-21, 2014 continuous manufacturing symposium, J. Pharm. Sci. 104 (2015) 803–812, https://doi.org/10.1002/jps.24324.
[7] K. Plumb, Continuous processing in the pharmaceutical industry: changing the mind set, Chem. Eng. Res. Des. 83 (2005) 730–738, https://doi.org/10.1205/cherd.04359.
[8] P. McKenzie, S. Kiang, J. Tom, A.E. Rubin, M. Futran, Can pharmaceutical process development become high tech? AICHE J. 52 (2006) 3990–3994, https://doi.org/10.1002/aic.11022.
[9] S.D. Schaber, D.I. Gerogiorgis, R. Ramachandran, J.M.B. Evans, P.I. Barton, B. L. Trout, Economic analysis of integrated continuous and batch pharmaceutical manufacturing: a case study, Ind. Eng. Chem. Res. 50 (2011) 10083–10092, https://doi.org/10.1021/ie2006752.
[10] A. Domokos, B. Nagy, B. Szilágyi, G. Marosi, Z.K. Nagy, Integrated continuous pharmaceutical technologies - a review, Org. Process. Res. Dev. 25 (2021) 721–739, https://doi.org/10.1021/acs.oprd.0c00504.
[11] A.G. Nambiar, M. Singh, A.R. Mali, D.R. Serrano, R. Kumar, A.M. Healy, A. K. Agrawal, D. Kumar, Continuous manufacturing and molecular modeling of pharmaceutical amorphous solid dispersions, AAPS PharmSciTech 23 (2022) 249, https://doi.org/10.1208/s12249-022-02408-4.
[12] B. Wood, K.P. Girard, C.S. Polster, D.M. Croker, Progress to date in the design and operation of continuous crystallization processes for pharmaceutical applications, Org. Process. Res. Dev. 23 (2019) 122–144, https://doi.org/10.1021/acs.oprd.8b00319.
[13] S. Mascia, P.L. Heider, H. Zhang, R. Lakerveld, B. Benyahia, P.I. Barton, R. D. Braatz, C.L. Cooney, J.M.B. Evans, T.F. Jamison, K.F. Jensen, A.S. Myerson, B. L. Trout, End-to-end continuous manufacturing of pharmaceuticals: integrated synthesis, purification, and final dosage formation, Angew. Chem. Int. Ed. 125 (2013) 12585–12589, https://doi.org/10.1002/ange.201305429.
[14] M.P. Meier, H.J.F. Bettin, K. Wohlgemuth, Understanding the effect of screw design on continuous particle isolation performance within a continuous vacuum screw filter, Powder Technol. 469 (2026) 121808, https://doi.org/10.1016/j.powtec.2025.121808.
[15] C. Steenweg, G. Schembecker, K. Wohlgemuth, Rotating-Screw Drying Reactor, , WO 2021/148108 A1 (, 2020.
[16] C. Steenweg, A.I. Seifert, G. Schembecker, K. Wohlgemuth, Characterization of a modular continuous vacuum screw filter for small-scale solid–liquid separation of suspensions, Org. Process. Res. Dev. 25 (2021) 926–940, https://doi.org/10.1021/acs.oprd.0c00550.
[17] C. Steenweg, A.I. Seifert, N. Böttger, K. Wohlgemuth, Process intensification enabling continuous manufacturing processes using modular continuous vacuum screw filter, Org. Process. Res. Dev. 25 (2021) 2525–2536, https://doi.org/10.1021/acs.oprd.1c00294.
[18] B. Hoffner, Ein neuartiges Verfahren zur Feststoffwaschung - Die Anwendung des Wanderbetts zur hochgradigen Aufreinigung partikulär-disperser Systeme. Dissertation, Karlsruhe, 2005.
[19] L.-M. Terdenge, Measurement and Control of Agglomeration for the Design of Crystalline Products. Dissertation, Dortmund, 2016.
[20] M. An, J. Qiu, D. Yi, H. Liu, S. Hu, J. Han, H. Huang, H. He, C. Liu, Z. Zhao, Y. Shi, P. Wang, Measurement and correlation for solubility of l-alanine in pure and binary solvents at temperatures from 283.15 to 323.15 K, J. Chem. Eng. Data 65 (2020) 549–560, https://doi.org/10.1021/acs.jced.9b00743.
[21] E.N. Constance, M. Mohammed, A. Mojibola, M. Egiefameh, O. Daodu, T. Clement, T. Ogundolie, C. Nwawulu, K. Aslan, Effect of additives on the crystal morphology of amino acids: a theoretical and experimental study, J. Phys. Chem. C 120 (2016) 14749–14757, https://doi.org/10.1021/acs.jpcc.6b04868.
[22] L. Hohmann, R. Gorny, O. Klaas, J. Ahlert, K. Wohlgemuth, N. Kockmann, Design of a continuous tubular cooling crystallizer for process development on lab-scale, Chem. Eng. Technol. 39 (2016) 1268–1280, https://doi.org/10.1002/ceat.201600072.
[23] C. Steenweg, A.C. Kufner, J. Habicht, K. Wohlgemuth, Towards continuous primary manufacturing processes - particle design through combined crystallization and particle isolation, Processes 9 (2021) 2187, https://doi.org/10.3390/pr9122187.
[24] A.C. Kufner, M. Meier, K. Wohlgemuth, End-to-end continuous small-scale drug substance manufacturing: from a continuous in situ nucleator to free-flowing crystalline particles, Crystals 13 (2023) 1675, https://doi.org/10.3390/cryst13121675.
[25] L. Hohmann, L. Löbnitz, C. Menke, B. Santhirakumaran, P. Stier, F. Stenger, F. Dufour, G. Wiese, S. zur Horst-Meyer, B. Kusserow, W. Zang, H. Nirschl, N. Kockmann, Continuous downstream processing of amino acids in a modular miniplant, Chem. Eng. Technol. 41 (2018) 1152–1164, https://doi.org/10.1002/ceat.201700657.
[26] N. Tonouchi, H. Ito, Present global situation of amino acids in industry, Adv. Biochem. Engin./Biotechnol. 159 (2017) 3–14, https://doi.org/10.1007/10_2016_23.
[27] M. Ding, S. Song, X. Li, A perspective on renewable production of amino acids from biomass through the chemocatalytic method, Green Chem. 26 (2024) 4468–4476, https://doi.org/10.1039/D4GC00846D.
[28] K. Wohlgemuth, Induced Nucleation Processes during Batch Cooling Crystallization. Dissertation, Dortmund, 2012.
[29] M.P. Meier, J. Marschner, C.I. Eicken, K. Wohlgemuth, Performance optimization of a continuous vacuum screw filter for various particle sizes by screw design, Powder Technol. (2026) (submitted).
[30] M.P. Meier, D.A. Rysch, K. Wohlgemuth, Replication Data for: Towards resource-efficient washing within the continuous vacuum screw filter, TUDOdata, 2026, https://doi.org/10.17877/TUDODATA-2026-JVFCSI.) V1. doi:.
[31] D. Jacobson-Kram, T. McGovern, Toxicological overview of impurities in pharmaceutical products, Adv. Drug Deliv. Rev. 59 (2007) 38–42, https://doi.org/10.1016/j.addr.2006.10.007.
[32] C. Steenweg, J. Habicht, K. Wohlgemuth, Continuous isolation of particles with varying aspect ratios up to thin needles achieving free-flowing products, Crystals 12 (2022) 137, https://doi.org/10.3390/cryst12020137.
[33] M.S. Ray (Ed.), Chemical Engineering, Volume 2: Particle Technology and Separation Processes, 4th edn, by J.M. Coulson and J.F. Richardson. Pergamon Press, Oxford, UK. 1991. (968 pp. ISBN 0–08–037957-5, John Wiley & Sons, Ltd, 1993).
[34] S. Tarleton, R. Wakeman, Solid/liquid separation: Equipment selection and process design, 1st ed., Elsevier/Butterworth-Heinemann, Amsterdam, 2007.
[35] R. Wakeman, The influence of particle properties on filtration, Sep. Purif. Technol. 58 (2007) 234–241, https://doi.org/10.1016/j.seppur.2007.03.018.
[36] H.S. Henn, F. Sauer, U.A. Peuker, B. Hoffner, Quantitative Beschreibung der partiellen Kuchenresuspendierung bei der Filterkuchenwäsche im Labormaßstab, Chem. Ing. Tech. 97 (2025) 23–31, https://doi.org/10.1002/cite.202300126.
[37] F. Ruslim, J. Fleischer, H. Nirschl, U. Peuker, Filterkuchenwäsche zur Aufreinigung löslicher kristalliner Feststoffpartikel, Chem. Ing. Tech. 78 (2006) 715–719, https://doi.org/10.1002/cite.200600011.
[38] H. Cao, C. Amador, X. Jia, Y. Ding, Capillary dynamics of water/ethanol mixtures, Ind. Eng. Chem. Res. 54 (2015) 12196–12203, https://doi.org/10.1021/acs.iecr.5b03366.
[39] S. Boduroglu, R. Bashir, Review of capillary rise experiments for surface-active solutes in the subsurface, Geotech 2 (2022) 706–730, https://doi.org/10.3390/geotechnics2030034.
[40] A.N. Gudkov, N.A. Fermor, N.I. Smirnov, Water - vapor pressure data, J.Appl. Chem.USSR 37 (1964) 2179–2184.
[41] A.N. Gudkov, N.A. Fermor, N.I. Smirnov, Water - vapor pressure data, Zh, Prikl. Khim. 37 (1964) 2204–2210.
[42] K.W. Chun, R.R. Davison, Thermodynamic properties of binary mixtures of triethylamine with methyl and ethyl alcohol, J. Chem. Eng. Data 17 (1972) 307–310, https://doi.org/10.1021/je60054a039.